International Journal of Refrigeration 170 (2025) 60–69

Contents lists available at ScienceDirect

International Journal of Refrigeration

journal homepage: www.elsevier.com/locate/ijrefrig

INSTITUT INTERNATIONAL DU FROID
INTERNATIONAL INSTITUTE OF REFRIGERATION

Heat transfer in large bins during the apples cool-down process

Transfert de chaleur dans les grandes caisses pendant le processus de refroidissement des pommes

Tuany Gabriela Hoffmann [a,b,*], Manfred Linke [a], Ulrike Praeger [a], Akshay D. Sonawane [a], Felix Büchele [c], Daniel Alexandre Neuwald [c,d], Reiner Jedermann [e], Barbara Sturm [a,b], Pramod V. Mahajan [a,**]

[a] *Department of Systems Process Engineering, Leibniz Institute for Agricultural Engineering and Bioeconomy (ATB), Potsdam, Germany*
[b] *Albrecht Daniel Thaer-Institute of Agricultural and Horticultural Sciences, Humboldt Universität zu Berlin, Berlin, Germany*
[c] *Lake of Constance Research Center for Fruit Cultivation (KOB), Ravensburg, Germany*
[d] *Department Production Systems of Horticultural Crops, University of Hohenheim, 70593 Stuttgart, Germany*
[e] *University Bremen, Institute for Microsensors, -actuators and -systems (IMSAS), Bremen, Germany*

ARTICLE INFO

Keywords:
Cold storage
Fruit preservation
Heat transfer
Horticultural produce
Malus domestica
Refrigeration

Mots clés:
Stockage frigorifique
Conservation des fruits
Transfert de chaleur
Produits horticoles
Malus domestica
Réfrigération

ABSTRACT

The preservation of apples in cold storage relies deeply on understanding the thermal dynamics governing their environment. Within packaging, apples engage in complex thermal interactions, between themselves and the environment, affecting convective and conductive heat transfer pathways. Challenges escalate in industrial cold storage facilities, manifesting as temperature stratification and non-uniform cooling. Nonetheless, a comprehensive understanding of heat transfer dynamics is vital for optimizing cold storage equipment design and enhancing cooling system operation efficacy. Building upon previous studies validating the use of Peltier elements for detecting and quantifying heat flux in individual apples, this research extends its application to industrial cold rooms. By strategically selecting locations within the apple bin and the storage cold room and comparing changes in total heat content obtained by a conventional method and comparing with the Peltier element for its validation. Results of the convective heat transfer coefficient in an upper-layer bin were in the range of 2.7-5.9 Wm^{-2} K^{-1} while in a bin at door level were 5.0-7.0 Wm^{-2} K^{-1}. The higher values found in the position near the door can be correlated to the faster air speed experienced between the apples in this position. By applying these values in the transient heat transfer model to predict the fruit core temperature during the cooling process, a relatable prediction was found, with apple temperature difference <0.9 °C between predicted by the Peltier element and experimental cooling curves. This study can aid understanding of thermal dynamics in cold storage environments, and support future development for more efficient and sustainable cold storage practices.

1. Introduction

In apple cold storage, the complex interplay of thermal phenomena influences the preservation of perishable commodities. Upon the introduction of fresh apples into cold storage environments, they are warmer compared to the surrounding air. This impacts the heat exchange mechanisms that comprise convection, conduction, and radiation. Apples act as hot bodies under the cooling phase, and the refrigeration system's function is to reduce the food temperature to enhance preservation (Chaomuang et al., 2019, Duan et al., 2020). Concurrently, the respiration process of apples causes a release of thermal energy (Hoffmann et al., 2021). The potential occurrence of phase changes, including transpiration (Bovi et al., 2018) and condensation (Linke et al., 2021), can take place depending on fruit and air conditions and affect the heat transfer.

Within the packaging, apples participate in multifaceted thermal interactions not only with the ambient air but also amongst themselves

* Corresponding author.
** Corresponding author at: Leibniz Institute for Agricultural Engineering and Bioeconomy (ATB), Max-Eyth-Allee 100 14469 Potsdam, Germany.
E-mail addresses: tuany.gabriela.hoffmann@student.hu-berlin.de (T.G. Hoffmann), pmahajan@atb-potsdam.de (P.V. Mahajan).

https://doi.org/10.1016/j.ijrefrig.2024.11.023
Received 21 August 2024; Received in revised form 8 October 2024; Accepted 16 November 2024
Available online 17 November 2024

Nomenclature

A	surface area [m^2]
Bi	Biot number [-]
c_p	heat capacity [J kg^{-1} K^{-1}]
Gr	Grashof number [-]
h_c	convective heat transfer coefficient [W m^{-2} K^{-1}]
L	diameter [m]
m	average mass [kg]
q	heat flux [W m^{-2}]
Q	heat content [J]
$\dot{Q}$	heat flow rate [W]
R	radius of apple [m]
Re	Reynolds number [-]
t	time [s]
$t_{7/8}$	seven-eighths cooling time [h]
T	Temperature [°C]
X	fraction [-]
Y	dimensionless temperature [-]

Greek symbols

λ	thermal conductivity [W m^{-1} K^{-1}]
ρ	density [kg m^{-3}]

Subscripts

a	air
b	bulk of apples
exp	experimental
i	initial
n	number of measurements
p	apple product
$pred$	predicted
s	apple surface
w	water

(Gruyters et al., 2018, Han et al., 2023), thereby affecting convective and conductive heat transfer pathways. The arrangement of apples in the bin creates a neighboring effect, impeding the free flow of air due to the proximity and contact between apples resulting in a preferred circulation of air within the bin and non-uniform heat dissipation (Wu et al., 2019). As the scale expands to industrial cold storage facilities, additional challenges are faced, such as the occurrence of temperature stratification (Han et al., 2021), which delineates regions of different thermal profiles characterized by localized thermal gradients.

To avoid the negative consequences of non-uniform cooling for fruits, strategies such as intensified air circulation are often used, although with associated risks including energy wastage (Wu et al., 2018) and potential damage to cellular integrity (Kongwong et al., 2019), accelerating food senescence. For fruits like apples, with 6 to 12 months storage in industrial cold rooms (Gross et al., 2016), a robust and precisely controlled refrigeration system is required. Due to simplified estimations of the heat load that accrues during storage, existing cold storage facilities face a significant issue, characterized by oversized equipment operating at partial loads, resulting in substantial energy waste. This inefficiency not only has economic implications but also contributes to environmental concerns (Evans et al., 2014, Boschiero et al., 2019, Büchele et al., 2024).

Taking into account the energy management and sustainability in food storage, a better comprehension of heat transfer between horticultural products and their immediate surroundings is needed to optimize packaging and design storage equipments, among other potential applications. In a previous study, the use of a small Peltier element to detect real-time heat flux between apples and environment during storage was introduced (Hoffmann et al., 2023). While this approach proved successful in validating its application with individual apples, the important need to extend its application to commercial cold rooms remains open and further research is needed.

In light of these considerations, this research aims to validate and extend the use of Peltier elements in industrial-level cold rooms to detect the heat flux between apples and their surrounding air during the initial cooling-down phase. For this purpose, two distinct locations, namely the upper-layer bin and the door-level bin, within the cold room were strategically selected. The heat transfer data obtained from the Peltier element at these locations was validated using a conventional method, and later, applied in a transient heat transfer model to predict fruit temperature during the cooling process. In addition, the airflow profile of the two chosen positions inside the cold rooms was investigated, alongside the cooling kinetics.

Table 1
Thermo-physical properties of apple.

Parameter	Value	Source
λ thermal conductivity [W m^{-1} K^{-1}][†]	0.406	Calculated
ρ_p apple density [kg m^{-3}]	837.22	Han et al. (2016)
ρ_b bulk of apples density [kg m^{-3}]	447.5	Measured
c_p heat capacity [J kg^{-1} K^{-1}]	3821.96	Han et al. (2016)
m mass [kg]	0.169 ± 0.003	Measured
L diameter [m]	0.071 ± 0.005	Measured
X_w water fraction/content [-]	0.868 ± 0.005	Measured

[†] Calculated based on the water fraction value, $\lambda = 0.322X_w + 0.1263$ (Donsi et al., 1996).

2. Materials and methods

2.1. Apples

Fresh apples (*Malus domestica* cv. Pinova) were collected during the 2023/2024 season at the Lake of Constance Research Center for Fruit Cultivation (KOB) in Southwestern Germany (47.76°N, 9.55°E). The harvesting was performed at the optimal harvest date in the region, starting from 4th October. The thermo-physical properties of the apple are presented in Table 1.

2.2. Cold storage

The measurements were carried out in a 50 t CA storage room at KOB in Ravensburg, Germany. The refrigeration system was installed by Kratschmayer Kälte-Klima-Lüftung GmbH (Kupferzell-Rüblingen, Germany), using propane (R290) as a fluid refrigerant (as recommended by the Regulation (EU) 2023/956 about the use of sustainable fluid refrigerants). The room was fully loaded with 157 standard bins (Agrar PA model, length × width × height = 1.20 m × 1.00 m × 0.76 m, material = high-density polyethylene, thermal conductivity = 0.40-0.49 W m^{-1} K^{-1}, thickness of side walls = 4 mm, total ventilation opening area (side and bottom perforation slots) = 0.223 m^2, CargoPlast GmbH, Salem, Germany) arranged in three rows of bin stacks. The bins were positioned inside the cold room maintaining circa 10 cm gap between bins along the tier, 10 cm along the rows, and 3 cm along the stacks. Each bin contained approximately 300 kg of apples. The room was filled uniformely with different varieties: ‘Cameo’, ‘Golden Delicious’,

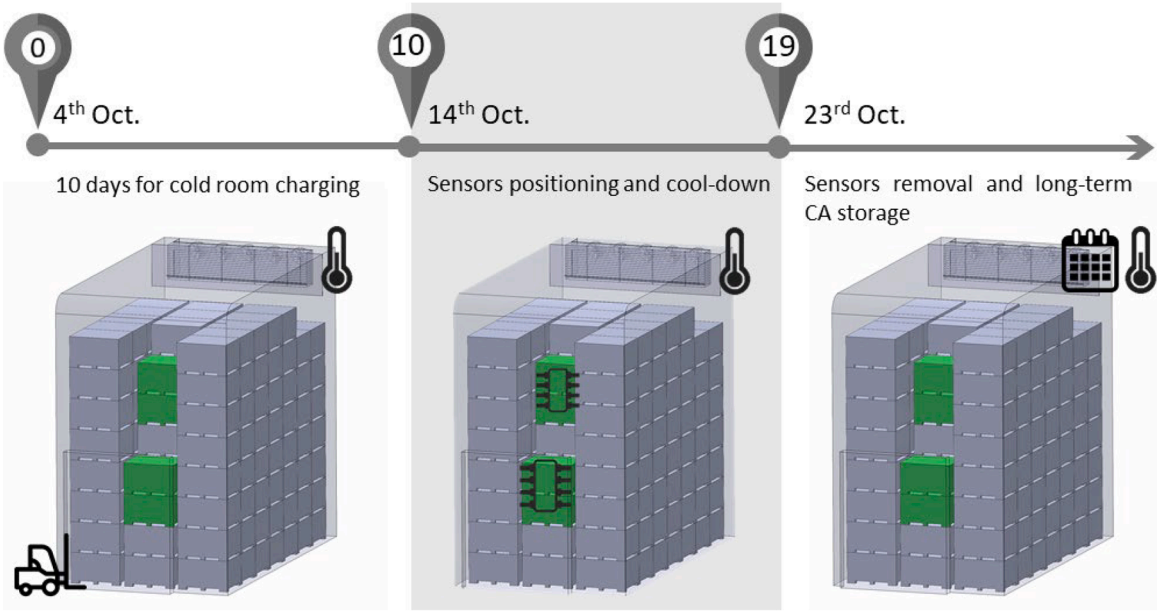

Fig. 1. Storage logistics regarding apples charging, sensors placement, cooling, and long-term controlled atmosphere (CA) storage.

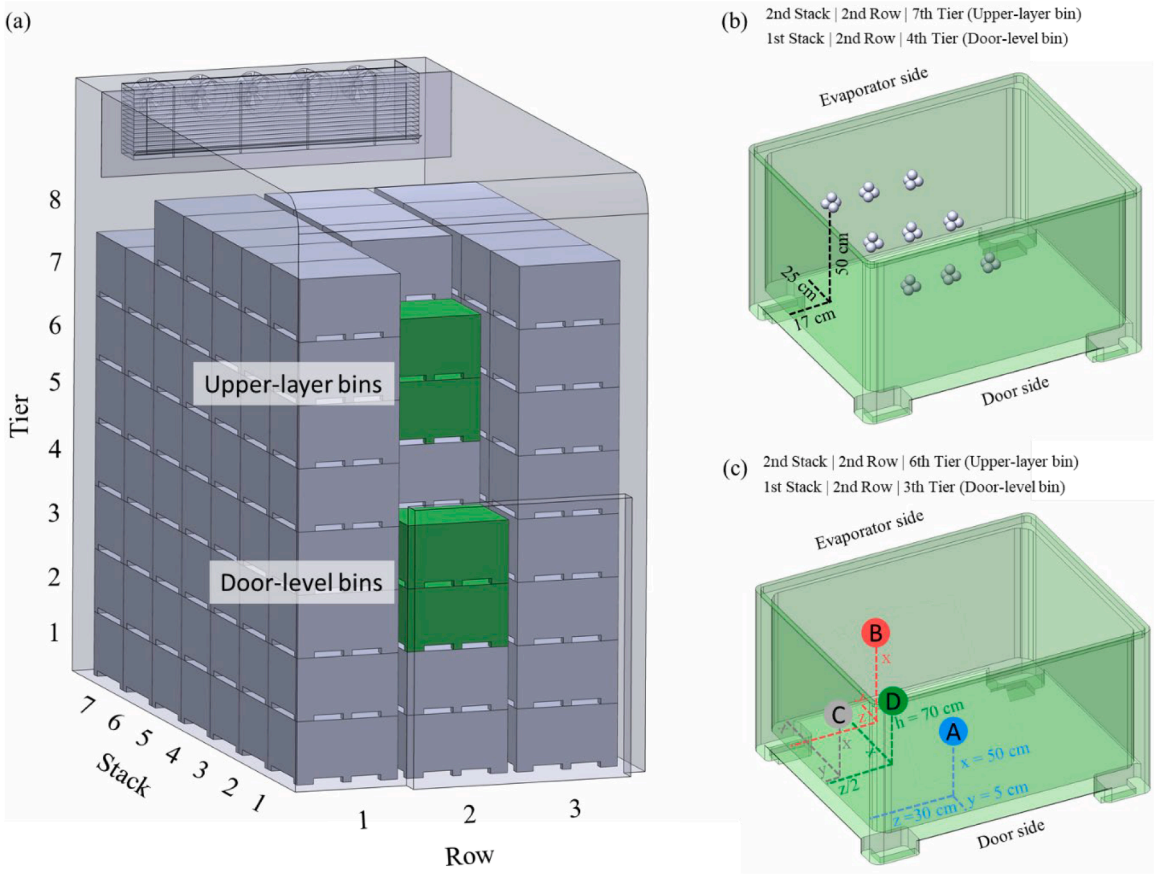

Fig. 2. (a) Identification of upper-layer and door-level postions. (b) Air speed sensors positions in half bin and the same plane. (c) Identification of the 4 measuring points inside one bin of apples, where sensors were placed at two different heights inside the same bin. Note: Due to the size of the cooling unit, stacks 6 and 7 can only have bins up to layer 7.

'Jonagold', 'Pinova', 'Elstar' and 'Red PrinceJonagold'. The results presented in this work are related to data collected with the apple cultivar 'Pinova'.

2.3. Experimental protocol

Apple storage started on 4th Oct. and spanned a period of 10 days to fully occupy the designated cold room. This period of charging the cold

room was selected to ensure that the bins of apples were added in uniform quantities daily and to simulate real storage logistic conditions. The refrigeration system operated since the first day of apple storage. On the final day of bin placement within the cold room (14th Oct.), sensors were strategically placed in four bins of apples, denoted by a green color in Fig. 1. The selected bins were positioned in two distinct locations: near the cold room door (door-level bin) and in the upper region of the stacked bins (upper-layer bin). For this reason, different cooling behaviors are expected. Sensors were distributed equally between the two locations (door-level bin and upper-layer bin), where one bin was designated to collect the air speed between apples (Fig. 2 b) while the second bin was responsible for the spatial temperature distribution and heat release (Fig. 2 c). The positioning of the sensors inside the bin considered the mirroring effect since the bins were positioned in the middle row of the cold room and presented equal distribution inside the cold room.

Data collection was conducted continuously for 9 consecutive days following the sensor deployment, with cooling conditions (1.0 ± 0.5 °C) and high relative humidity (> 90 % after the first day of storage) maintained throughout the entire process. Additionaly, 1-Methylcyclopropene (SmartFresh™ ProTabs, AgroFresh Co., Philadelphia, PA, USA) treatment was applied to enhance the preservation of fruits during this period. After this period, sensors were removed from the bin of apples. The cold room was then sealed, and controlled atmosphere (CA) storage conditions (1 kPa O_2 and 2.5 kPa CO_2) were implemented for the long-term preservation of the stored apples.

2.4. Cooling kinetics analysis

Based on the apple and air temperature profiles, both collected with film thermistors (MF5B, Jinlongbao Electronic Co., Guangdong, China) 5-point calibrated for the temperature range of interest (0 to 25 °C) using a temperature calibrator EP21 (SIKA, Kaufungen, Germany), the dimensionless temperature (Y) was calculated as Eq. (1).

$$Y(t) = \frac{T_P(t) - T_a(t)}{T_{p,i} - T_a(t)} \tag{1}$$

where T_a is the air temperature (cooled air from the cooling unit), $T_{p,i}$ is the initial apple core temperature and T_P is the apple core temperature at time t. From Y, the seven-eighths cooling time ($t_{7/8}$) was calculated. The $t_{7/8}$ corresponds to the time required to reduce (pull down) the difference between the fruit and air temperature by Y equals 0.125.

The average dimensionless temperature (Y^*) of n apples was determined as Eq. (2). For this purpose, 4 different positions were considered inside the same bin of apples, as shown in Fig. 2 c. Positions A, B, and C were placed 50 cm above the floor of the bin while position D was on the top layer of apples (70 cm above the floor of the bin). A and B were in equidistance along the half bin length and apart from the bin wall by 5 cm. Position C was in equidistance along the bin width and also apart from the bin wall in 5 cm. Position D was positioned in a center position, considering a half bin.

$$Y^*(t) = \frac{1}{n}\sum_{i=1}^{n} Y_i(t) \tag{2}$$

2.5. Heat flux measurements

The heat flux of the fruit was assessed utilizing Peltier elements (PE) (TEC1-00706, Hebei Yuxiang Electronics Co., Zhangjiakou, China) affixed to the fruit surface. In a prior investigation by Hoffmann et al. (2023), the real-time heat flux between individual fruits and their environment in different postharvest scenarios was determined. The same methodology was replicated in the current study to determine the heat flux within the bin at four distinct positions. Two PEs, each measuring 10 mm × 10 mm × 4 mm (length × width × thickness), were strategically positioned 180° apart along the circumference of the fruit's surface and placed at the surface geometrical center of the fruit. This arrangement aimed to obtain a representative mean heat flux value for a single apple. Thermal glue (EC360GLUE, Jaden Technologies, Duisburg, Germany) was employed to attach the PEs onto the apple surface. Heat flux data from PE was adjusted using a certified heat flux sensor (HFS-5, temperature range from -50 to 120 °C, Omega Engineering, Deckenpfronn, Germany).

2.6. Validation of PE for heat flux measurement

In order to validate the heat flux measurements acquired with the PE, a conventional method for determining heat flux based on the heating and cooling curves was used as a comparison (Hoffmann et al., 2023). This method operates on the premise that the heat content (Q, in J) of the fruit can be determined using Eq. (3).

$$Q = mc_p\Delta T \tag{3}$$

where m represents mass in kg, c_p is the specific heat in J kg^{-1} K^{-1} and ΔT is the temperature difference between the fruit and a reference temperature (°C) (Singh and Heldman, 2009).

The heat flow rate ($\dot{Q}$, in W) is defined as the quantity of heat transferring from a region of higher temperature to one of lower temperature per unit time (t), as expressed in Eq. (4).

$$\dot{Q} = Q/\Delta t \tag{4}$$

The heat flux (q, in W m^{-2}) is calculated from the heat flow rate related to the exchange area (A, in m^2), as follows

$$q = \dot{Q}/A \tag{5}$$

When combining Eqs (3) and (4) into Eq. (5), the correlation for heat flux based on the change in average fruit temperature is obtained as expressed in Eq. (6).

$$q = \left(mc_p\Delta T\right)/\left(A\Delta t\right) \tag{6}$$

For validation, the heat flux values obtained with the PE were compared with heat flux calculated based on the methodology described previously, considering the same amount of time.

2.7. Model for predicting apple temperature

The convective heat transfer coefficient (h_c, in W m^{-2} K^{-1}) was determined from the heat flux data by applying Eq. (7), which follows the Newton's law of cooling.

$$h_c = q/(T_a - T_s) \tag{7}$$

where q is the heat flux in W m^{-2}, T_a is the air temperature and T_s is the fruit surface temperature, both temperature measurement in°C. For the fruit surface temperature, a digital non-contact infrared thermal sensor (MLX 90416, Melexis Technologies, Tessenderlo, Belgium) was positioned 10 mm from the apple peel. The sensor was calibrated for the temperature range of interest (0 to 25 °C) using a temperature calibrator EP21 (SIKA, Kaufungen, Germany).

In order to determine the core temperature of the apples, the average h_c value for each bin obtained based on the Peltier element data was implemented in a simple model for estimating the core temperature evolution of regular-shaped food products. The model, established by van der Sman (2003) and successfully employed by Duret et al. (2014) and Laguerre et al. (2022), enables the calculation of the average temperature of high-moisture food products with or without evaporation (Eq. (8)).

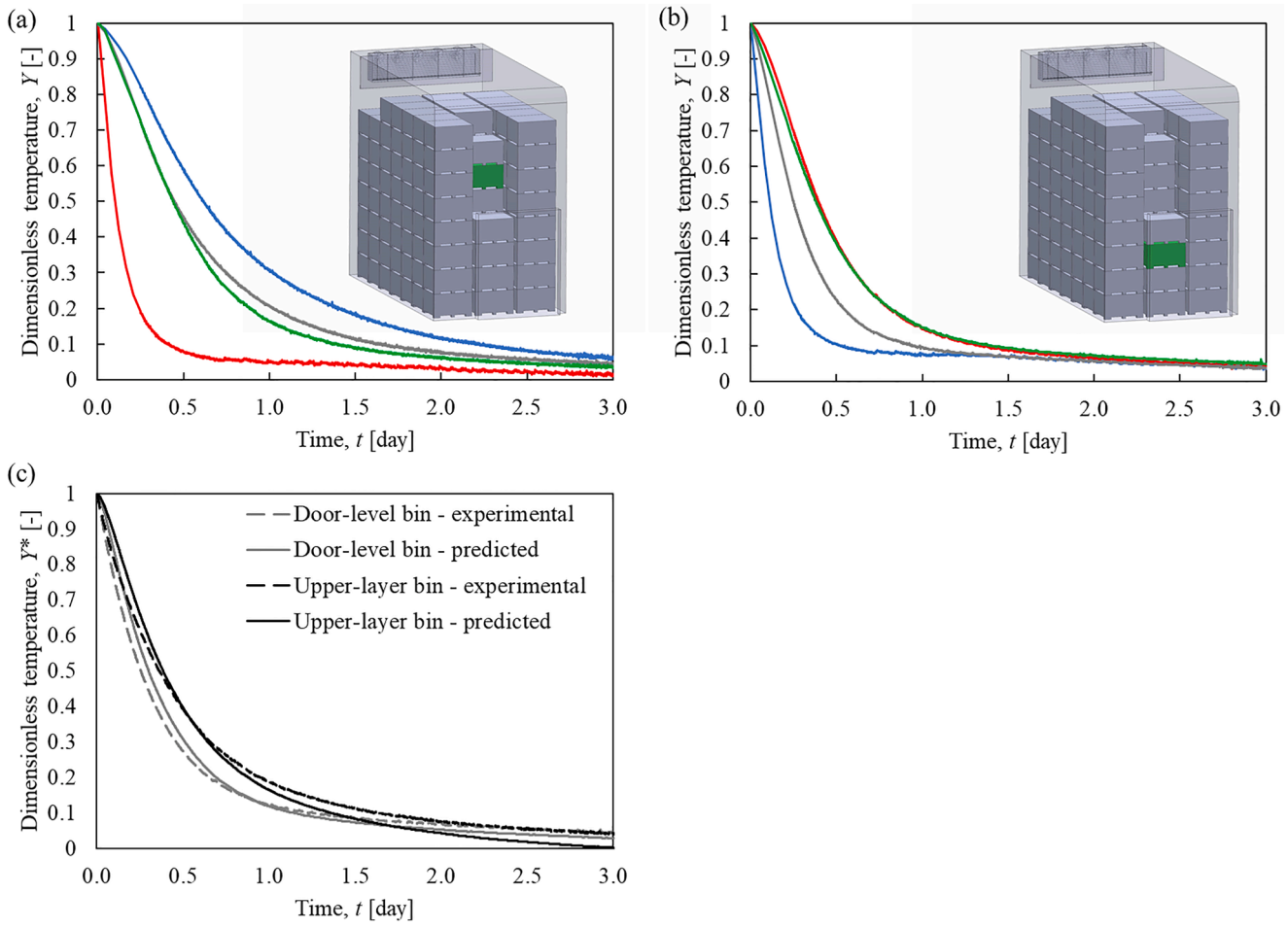

Fig. 3. Dimensionless temperature in different positions inside the bin placed on the (a) upper-layer bin, (b) door-level bin, and (c) comparison between the average dimensionless temperature curves of each bin and predicted curve by the transient heat transfer model.

$$mc_p\frac{dT_p(t)}{dt} = A\frac{(T_a(t) - T_p(t))}{\left(\frac{1}{h_c} + \frac{R}{4\lambda}\right)} \tag{8}$$

where R is the radius of the apple and A is the fruit surface area (calculated as a function of the mass, $A = 0.0581m^{0.685}$, Clayton et al. (1995)). Eq. (4) was solved using a fourth-order Runge-Kutta method (Python 3.12, Python Software Foundation). This transient heat transfer model is acceptable for $Bi < 10$. Respiration heat was not included due to its low value (15-21 W ton^{-1} at 5 °C, ASHRAE (2014)). The exchange of radiation heat is expected to be limited compared to convection heat transfer, given the small temperature difference (typically < 1 °C) between neighboring apples during cooling.

Table 2
Cooling times and heat transfer coefficient results for the upper-layer bin and door-level bin.

Bin position	Sensor position†	$t_{7/8}$ [day]	h_c [W m^{-2} K^{-1}]
Upper-layer	A	1.90	2.7
	B	0.34	5.9
	C	1.41	5.6
	D	1.20	4.3
	Average	1.21	4.6
Door-level	A	0.41	7.0
	B	1.12	5.0
	C	0.78	6.7
	D	1.15	5.1
	Average	0.86	5.9

† Identification as in Fig. 2 c.

The Root Mean Square Error (*RMSE*), as presented in Eq. (9), was used to statistically analyze the differences between the experimental ($T_{p,exp}$) and predicted fruit produce temperature ($T_{p,pred}$).

$$RMSE = \sqrt{\frac{\sum_{i=1}^{n}\left(T_{p,pred} - T_{p,exp}\right)^2}{n}} \tag{9}$$

For this analysis, the number of measurements (n) taken into account was equal to 800, considering the cool-down process until stable conditions.

2.8. Air flow measurement

The air speed logger device, as developed by Geyer et al. (2018) for quantifying omnidirectional air speed in macroporous media, was utilized in this study. It is important to highlight that this device characterizes air movement with an unknown direction between the apples, therefore, the results are presented as air speed. It comprises four hollow transparent spheres made of polystyrene, arranged in a pyramidal array similar to the physical arrangement of bulky fruit. The device has a detection range for air speed between 0 to 1.5 m s^{-1}, estimated between apples inside the bin (Praeger et al., 2020). Silicon diodes fixed between the spheres in free space enable air speed measurement based on a calorimetric principle. Nine devices were used per bin (upper-layer bin and door-level bin) to record air speed at various points within the bin, as illustrated in Fig. 2. The sensors were distributed in equal distances on half bin, in the same plane, and placed 50 cm above the floor of the bin

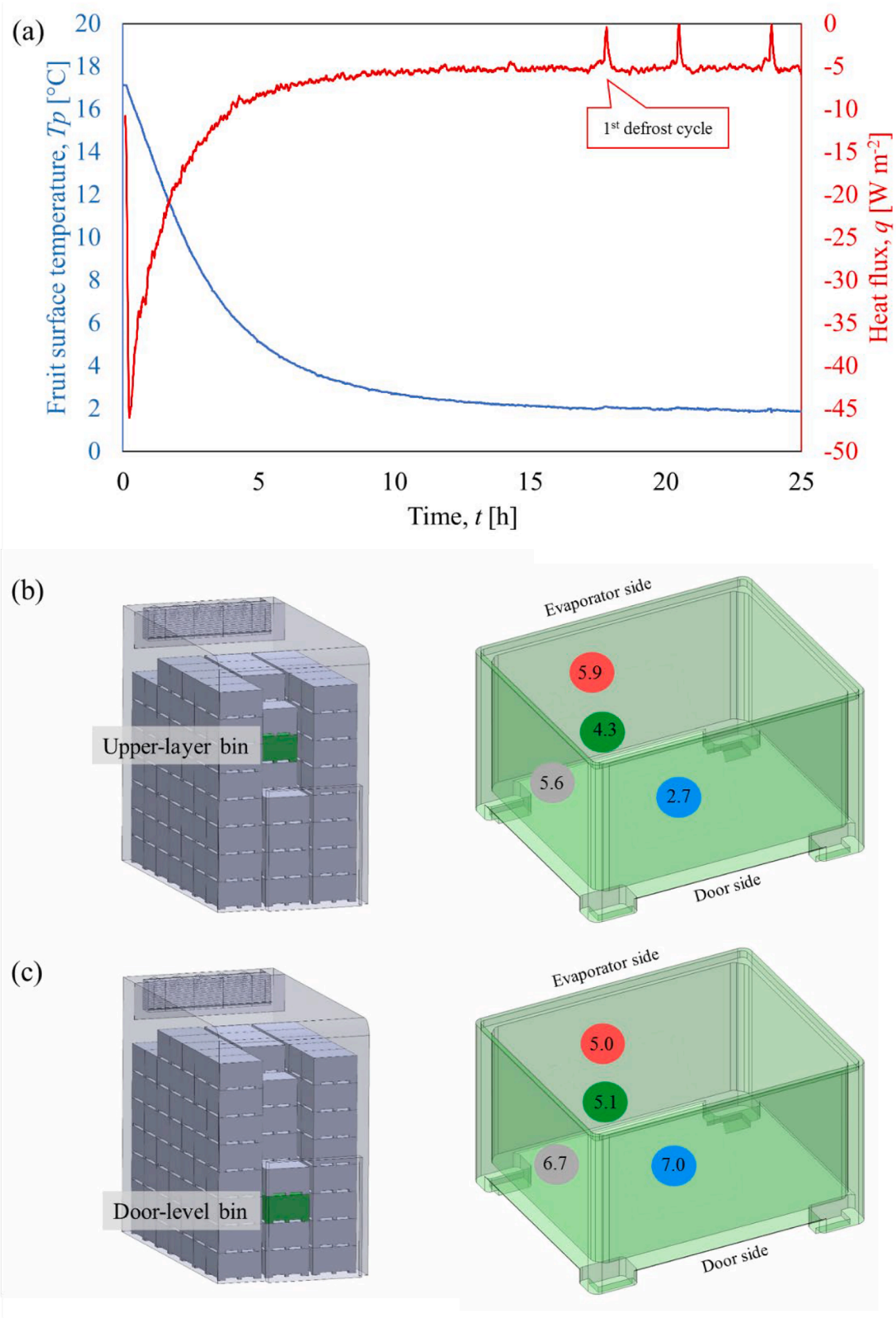

Fig. 4. (a) Heat flux profile according to the fruit surface temperature. Convective heat transfer coefficient (h_c) values in the (b) upper-layer bin and (c) door-level bin inside the cold room. Results of h_c are presented in W m^{-2} K^{-1}.

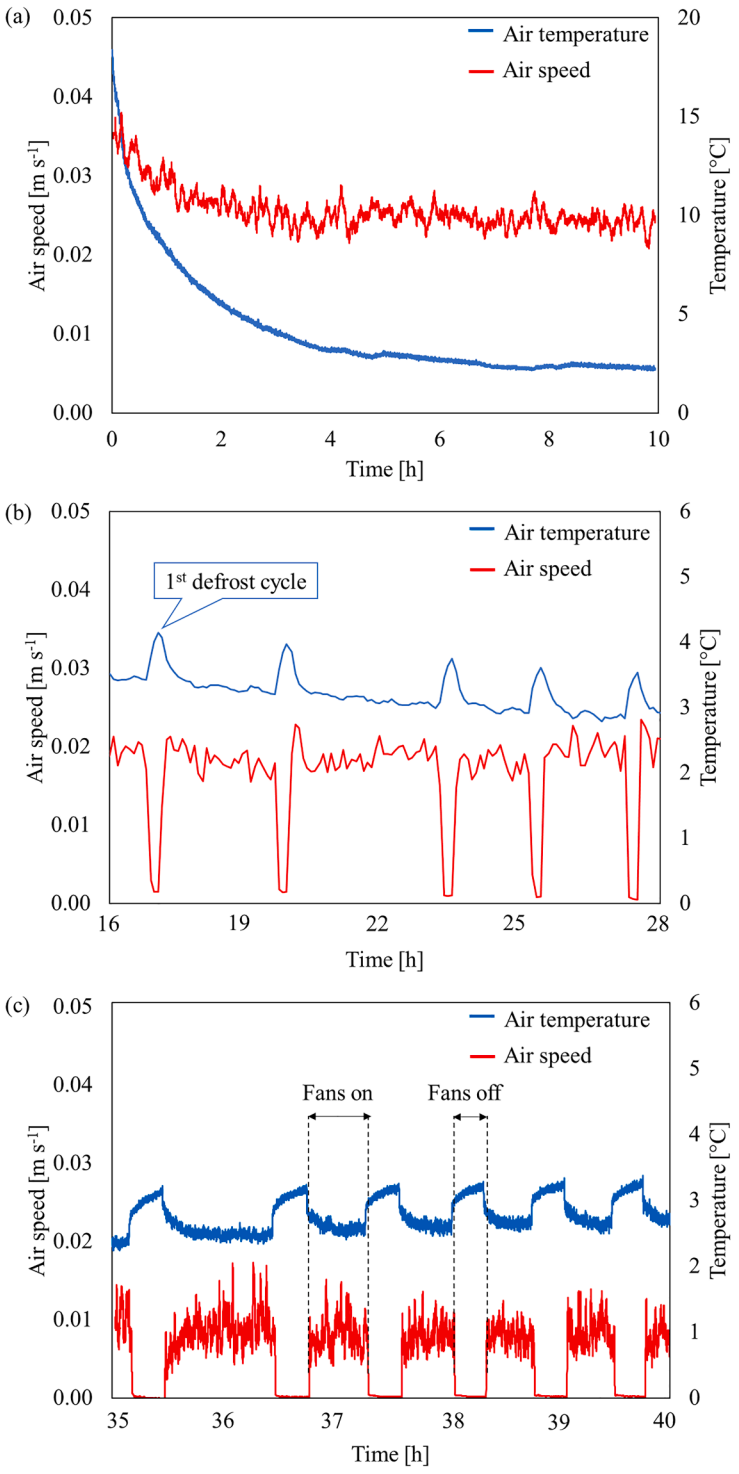

Fig. 5. Air speed and air temperature between the apples inside the bin during (a) cool-down process (first day of bin of apples cooling), (b) end of coold-down process and (c) under stable air temperature. Data from upper-layer bin and the center position sensor.

(Fig. 2 b).

3. Results and discussion

3.1. Cooling kinetics analysis

The dimensionless temperature (Y) for four different positions inside the bin of apples and in different areas inside the cold room are presented in Fig. 3 a and b. The upper-layer bin is more influenced by the cooled airflow on the bin's side facing the evaporator (red curve), presenting $t_{7/8}$ equal to 0.34 day, followed by the centralized position at the top layer of apples (green curve, $t_{7/8}$ = 1.20 day), center position according to the bin's width (grey curve, $t_{7/8}$ = 1.41 day), and lastly, the opposite position to the incoming air from the evaporator (blue curve, $t_{7/8}$ = 1.90 day) (Table 2). The opposite was observed at the door-level bin (Fig. 3 b). The faster position to cool down was found at the bin's side facing the cold room door (blue curve, $t_{7/8}$ = 0.41 day), which could

be attributed to the larger gap for air to flow in this region when compared with the gaps between the bins along the stacks.

Seven-eighths cooling time ($t_{7/8}$) was obtained by analyzing the temperature evolution during the pull-down process and is presented in Table 2. Short cooling times were found at the door-level bin (average $t_{7/8}$ equal to 0.86 day) when compared to the upper-layer bin (average $t_{7/8}$ equal to 1.21 day). This can be a result of the higher air speed registered at the door-level bin, providing faster cooling.

3.2. Heat flux within bin

Heat flux denotes the rate of heat transfer per unit area, playing a crucial role in determining how rapidly an apple sheds heat to its surroundings. When the apple's temperature exceeds that of its environment, heat moves from the apple to the surroundings due to the temperature differential (Hoffmann et al., 2023). Fig. 4 a shows the heat flux profile during the cooling process of an apple within a bin. At the beginning of the apple cool-down, an outgoing heat flux of 46.1 W m^{-2} was reported while a value slightly close zero was observed after apple temperature stability, which can be an effect of neighboring apples and/or the water removal from the apple assisted by evaporative heat due to the respiration mechanism. In packed beds, the intensity of heat transfer is position-dependent (Alvarez et al., 1999). Heat transfer diminishes in accordance with the airflow velocity along the packed bed. Furthermore, heat transfer decreases near the bin walls where there are no perforations. This phenomenon can be attributed to a local variation in the void fraction within the bed, resulting in fluctuations in the interstitial velocity (Wakao and Kaguei, 1982).

The heat content of the apples, to reduce fruit temperature from 16 °C (temperature before cooling) to 1 °C, was calculated according to Eq. (3) and the values were found as circa 10 kJ. During the cooling process, this amount of heat is released and can be estimated by the PE. For each PE position inside the bin, the amount of heat released through the area of the PE was determined. Results showed a deviation <4.9 % from the value obtained with PE when compared with values previously calculated (Eq. (3)). The PE can be used as a tool for determining the thermal profile of single apples as well as bulk of apples during cooling process, under free and forced convection (Hoffmann et al., 2024). By directly recording the incoming and outgoing heat flows, the PE provides critical insights into how temperature fluctuations affect fruit and vegetable quality. This method also takes into account essential factors like air velocity and radiation, leading to a more comprehensive understanding of postharvest temperature dynamics and their impact on product preservation. In the context of cold storage, this precise thermal data is essential for optimizing environmental parameters, thereby reducing energy consumption and minimizing temperature heterogeneities within the storage environment.

From the heat flux data of apples inside the bin and Eq. (7), the h_c values for four different positions within the bin, and in the upper-layer bin and door-level bin, inside the cold room are presented in Fig. 4 b and c, respectively. In the upper-layer bin, the h_c values were in the range from 2.7 to 5.9 W m^{-2} K^{-1} while the door-level bin was 5.0 to 7.0 W m^{-2} K^{-1}, with respective average values of 4.6 W m^{-2} K^{-1} and 5.9 W m^{-2} K^{-1}. The higher values in the position near the door can be correlated to the faster air speed experienced between the apples in this position. The h_c is directly related to the airflow impinging the apples inside the bin, which affects the apple thermal dynamics according to Newton's Law of Cooling (Incropera and DeWitt, 1990).

3.3. Apple temperature prediction

The average h_c values, obtained from Peltier element measurements, for the upper-layer bin (4.6 W m^{-2} K^{-1}) and the door-level bin (5.9 W m^{-2} K^{-1}), were applied to the transient heat transfer model (Eq. (8)) to predict the fruit temperature (T_p) during the cooling process. Fig. 3 c compares the average dimensionless temperature (Y^*) predicted by the model and the experimental measurements. The predictive trends align well with acceptable consistency, with the *RMSE* for the product temperature < 0.9 °C. At the beginning of cooling, the predicted curves for the upper-layer bin and door-level bin presented a slight delay in temperature reduction, nevertheless, a similar temperature reduction profile was observed. These findings further validate the use of the PE methodology applied for determining the heat fluxes between apples and their sorroundings, where the h_c can be derivated.

3.4. Air flow profile

The air circulation inside the cold room not only facilitates the removal of heat from the stored items but also plays a crucial role in maintaining a uniform temperature distribution within the storage system. During the cool-down process, the fans remained in operation continuously (up to 16 h), at constant power, until temperature difference of almost 2-3 K remains between the set value (1 °C) at the cooling unit and the air temperature inside the bin, as observed in Fig. 5 a and b, where the air speed inside the bin is shown according to time and air temperature pull-down.

The compressor on-off strategy has a direct effect on air temperature fluctuation, providing a cyclical profile. This cycle unfolds in two distinct stages. In the initial stage, when the compressor activates, the mean air temperature decreases to its minimum value. Subsequently, in the second stage, when the compressor deactivates, the mean air temperature rebounds from its minimum to the maximum value. This cyclical pattern displays a fluctuating temperature profile, as illustrated in Fig. 5 b and c. Notably, during the compressor's off period (rewarming phase), the fans remain inactive for approximately 20 minutes. Fig. 5 b demonstrates that despite the fans being deactivated during the initial defrosting cycle, the detected air speed inside the bin was not zero. This phenomenon can be attributed to the occurrence of free convection, which arises from temperature gradients within the bin and drives vertical air movement. In addition, during the cool-down phase some air speed variation inside the bin is observed (Fig. 5 a), reducing from nearly 0.04 to 0.02 m s^{-1}, although the fans were operating under constant power during this period. Highlighting once again the presence of free convection while cooling the apples.

In the cooling phase, the free convection airflow is directed vertically, from the bottom to the top. Conversely, the forced convection airflow primarily travels horizontally from the door towards the cooling unit. The intensity of the free convection airflow decreases as the temperature differential between the fruit surface and the cold air diminishes. In contrast, the forced convection airflow remains constant unless significantly impeded by evaporator icing. Consequently, variations in air speed at the measurement locations are due to the interplay between these superimposed airflows, which can either obstruct or enhance each other. Moreover, the forced convection airflow will preferentially follow the path of least resistance (such as the gaps between the bins), maintaining a horizontal direction. Important to highlight that these findings only apply to the cooling-down phase.

When comparing both positions inside the cold room (upper-layer bin and door-level bin), the door-level bin presented faster air speed between the apples in central position in the bin, which can be a result of the vertical flow. This can be an indication of presence of free convection effect, leading to the understandment that both, free and forced convections, acted during the intial cooling phase of apples inside the cold room. In the specific experimental conditions, the Gr/Re^2 values favor free convection, further emphasizing the prevalence of free convection characteristics (Baehr and Stephan, 2011).

The upper-layer bin has a air speed indication of horizontal airflow through the bin. This pattern can be explained by the forced air movement provided by the cooling unit. Cooled air leaves the cooling unit and flows over the bins directly to the opposite corner, in a predominantly horizontal flow. As it approaches the opposite wall, the air velocity

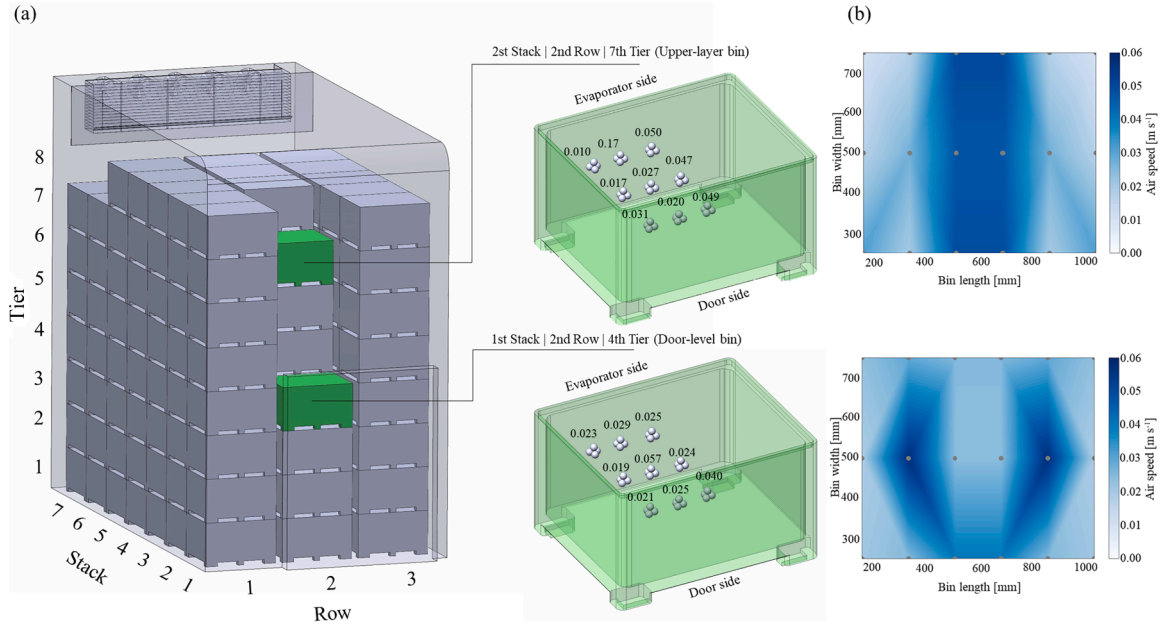

Fig. 6. (a) Air speed inside the bin of apple in two different positions inside the cold room (upper-layer bin and door-level bin). (b) Counter map of the air speed profile inside the bin, according to mirroring effect.

gradually decelerates. Subsequently, the air undergoes a shift in direction, adopting a primarily vertical flow as it flows through the stacked produce while returning to the cooling unit and taking heat from the produce. The air movement pattern inside the cold room is already well-established in the literature (Ambaw et al., 2016, Praeger et al., 2020, Han et al., 2021), however, more information regarding the air speed inside the bin is needed to better comprehend the heat transfer due to air movement (free and/or forced convection).

The air speed inside the bin of apples showed variations up to 51 % from the average value (Fig. 6), considering measurements at 9 different positions inside one bin. In the upper-layer bin, the minimum air speed was 0.010 m s^{-1} and the maximum air speed 0.050 m s^{-1}, while the door-level bin presented 0.019 m s^{-1} and 0.057 m s^{-1}, respectively. Average values were 0.030 m s^{-1} for the upper-layer bin and 0.029 m s^{-1} for the door-level bin.

4. Conclusion

In this study by extension of a previous study to apply Peltier elements for detecting heat flux in individual apples, their application in industrial cold rooms was demonstrated and validated. The close agreement between predicted and experimental cooling curves (< 0.9 °C of fruit temperature difference) further reinforces the utility of this methodology. The findings, including the determination of convective heat transfer coefficients at different locations within the cold room (upper-layer and door-level bins) and comprehension of cooling kinetics offer valuable insights into optimizing cold storage equipment design and improving cooling efficacy. Additionally, the superimposition and synergy of free and forced convection in a partially closed enclosure (packed bed of apples inside a bin) were observed during the cool-down phase, indicating that both types of convection should be considered during the cooling process. Overall, this research not only contributes to the build of knowledge on thermal dynamics in cold storage environments but also lays a foundation for future developments aimed at enhancing efficiency and sustainability in cold storage practices.

CRediT authorship contribution statement

Tuany Gabriela Hoffmann: Writing – original draft, Methodology, Investigation, Data curation, Conceptualization. **Manfred Linke:** Writing – review & editing, Investigation. **Ulrike Praeger:** Writing – review & editing, Investigation, Funding acquisition. **Akshay D. Sonawane:** Writing – review & editing. **Felix Büchele:** Writing – review & editing. **Daniel Alexandre Neuwald:** Writing – review & editing. **Reiner Jedermann:** Writing – original draft, Investigation. **Barbara Sturm:** Writing – review & editing, Supervision. **Pramod V. Mahajan:** Writing – review & editing, Supervision, Project administration.

Declaration of competing interest

The authors declare that they have no known competing financial interests or personal relationships that could have appeared to influence the work reported in this paper.

Acknowledgements

The authors gratefully acknowledge the support of the Landwirschaftliche Rentenbank, Germany [grant number 1007860] in the research project “DyNatCool - Transformation of cold management and refrigeration of fruit storage rooms into the digital age by means of simulative and practical system comparison”. The authors thank in particular Stefan Elwert (ATB) for his support in the preparation of the drawings for the manuscript and Daniel Dadej (KOB) and Lukas Dadej (KOB) for support in harvesting the apples and arranging the bins in the cold room.

References

Alvarez, G., Flick, D., 1999. Analysis of heterogeneous cooling of agricultural products inside bins Part II: thermal study. J. Food Eng. 39, 239–245. https://doi.org/10.1016/S0260-8774(98)00166-6.

Ambaw, A., Bessemans, N., Gruyters, W., Gwanpua, S.G., Schenk, A., de Roeck, A., Delele, M.A., Verboven, P., Nicolai, B.M., 2016. Analysis of the spatiotemporal temperature fluctuations inside an apple cool store in response to energy use concerns. Int. J. Refr. 66, 156–168. https://doi.org/10.1016/j.ijrefrig.2016.02.004.

ASHRAE, 2014. *ASHRAE Handbook - Fundamentals*. Chapter 10: Cooling and Freezing Times of Foods. ASHRAE, Atlanta.

Baehr, H.D., Stephan, K., 2011. Heat and Mass Transfer. Springer Berlin, Heidelberg. https://doi.org/10.1007/978-3-642-20021-2.

Boschiero, M., Zanotelli, D., Ciarapica, F.E., Fadanelli, L., Tagliavini, M., 2019. Greenhouse gas emissions and energy consumption during the post-harvest life of

apples as affected by storage type, packaging and transport. J. Clean. Prod. 220, 45–56. https://doi.org/10.1016/j.jclepro.2019.01.300.
Bovi, G.G., Rux, G., Caleb, O.J., Herppich, W.B., Linke, M., Rauch, C., Mahajan, P.V., 2018. Measurement and modelling of transpiration losses in packaged and unpackaged strawberries. Biosyst. Eng. 174, 1–9. https://doi.org/10.1016/j.biosystemseng.2018.06.012.
Büchele, F., Hivare, K., Khera, K., Thewes, F.R., Argenta, L.C., Hoffmann, T.G., Mahajan, P.V., Prange, R.K., Pareek, S., Neuwald, D.A., 2024. Novel energy-saving strategies in apple storage: a review. Sustainability 16, 1052. https://doi.org/10.3390/su16031052.
Chaomuang, N., Flick, D., Denis, A., Laguerre, O., 2019. Experimental analysis of heat transfer and airflow in a closed refrigerated display cabinet. J. Food Eng. 244, 101–114. https://doi.org/10.1016/j.jfoodeng.2018.09.009.
Clayton, M., Amos, N.D., Banks, N.H., Morton, R.H., 1995. Estimation of apple fruit surface area. New Zeal. J.Crop Hort. Sci. 23, 345–349. https://doi.org/10.1080/01140671.1995.9513908.
Donsi, G., Ferrari, G., Nigro, R., 1996. Experimental determination of thermal conductivity of apple and potato at different moisture contents. J. Food Eng. 30, 263–268. https://doi.org/10.1016/S0260-8774(96)00044-1.
Duan, Y., Wang, G.-B., Fawole, O.A., Verboven, P., Zhang, X., Wu, R., Opara, D., L, U., Nicolai, B., Chen, K, 2020. Postharvest precooling of fruit and vegetables: A review. Trends. Food Sci. Technol. 100, 278–291. https://doi.org/10.1016/j.tifs.2020.04.027.
Duret, S., Hoang, H.-M., Flick, D., Laguerre, O., 2014. Experimental characterization of airflow, heat and mass transfer in a cold room filled with food products. Int. J.Refr. 46, 17–25. https://doi.org/10.1016/j.ijrefrig.2014.07.008.
Evans, J.A., Hammond, E.C., Gigiel, A.J., Fostera, A.M., Reinholdt, L., Fikiin, K., Zilio, C., 2014. Assessment of methods to reduce the energy consumption of food cold stores. Appl. Therm. Eng. 62, 697–705. https://doi.org/10.1016/j.applthermaleng.2013.10.023.
Geyer, M., Praeger, U., Truppel, I., Scaar, H., Neuwald, D.A., Jedermann, R., Gottschalk, K., 2018. Measuring device for air speed in macroporous media and its application inside apple storage bins. Sensors 18, 576. https://doi.org/10.3390/s18020576.
Gross, K.C., Wang, C.Y., Saltveit, M., 2016. The Commercial Storage of Fruits, Vegetables, and Florist and Nursery Stocks. Agriculture Handbook 66. U.S. Department of Agriculture, Agricultural Research Service, Washington, DC.
Gruyters, W., Verboven, P., Diels, E., Rogge, S., Smeets, B., Ramon, H., Defraeye, T., Nicolai, B.M., 2018. Modelling cooling of packaged fruit using 3D shape models. Food Bioproc. Tech. 11, 2008–2020. https://doi.org/10.1007/s11947-018-2163-9.
Han, J.-W., Zhao, C.-J., Yang, X.-T., Qian, J.-P., Fan, B.-L., 2016. Computational modeling of airflow and heat transfer in a vented box during cooling: optimal package design. Appl. Therm. Eng. 91, 883–893. https://doi.org/10.1016/j.applthermaleng.2015.08.060.
Han, J.-W., Ji, Z.-T., Zou, M., Yang, X.-T., 2021. Integral evaluation for intermittent cold storage of apples by using mathematical modeling. J. Food Process. Eng. 44, e13882. https://doi.org/10.1111/jfpe.13882.
Han, J.-W., Ren, Q.-S., Li, J.-C., Zhu, W.-Y., Yang, X.-T., 2023. Numerical analysis of coupled heat and mass transfer processes in packaged tomatoes throughout the cold chain. Case Stud. Therm. Eng. 42, 102687. https://doi.org/10.1016/j.csite.2022.102687.
Hoffmann, T.G., Ronzoni, A.F., da Silva, D.L., Bertoli, S.L., de Souza, C.K., 2021. Cooling kinetics and mass transfer in postharvest of fresh fruits and vegetables under refrigerated conditions. Chem. Eng. Trans. 87, 115–120. https://doi.org/10.3303/CET2187020.
Hoffmann, T.G., Mahajan, P.V., Praeger, U., Geyer, M., Sturm, B., Linke, M., 2023. Small Peltier element to detect real-time heat flux between apple and environment during postharvest storage. Comput. Electron. Agric. 213, 108247. https://doi.org/10.1016/j.compag.2023.108247.
Hoffmann, T.G., Praeger, U., Mahajan, P., Geyer, M., Jedermann, R., Linke, M., 2024. Peltier element for real-time heat flux detection in fruit cooling under forced air convection. Acta Hortic. 1396. https://doi.org/10.17660/ActaHortic.2024.1396.38.
Incropera, F.P., DeWitt, D.P., 1990. Fundamentals of Heat and Mass Transfer. John Wiley and Sons, New York.
Kongwong, P., Boonyakiat, D., Poonlarp, P., 2019. Extending the shelf life and qualities of baby cos lettuce using commercial precooling systems. Postharvest Biol.Technol. 150, 60–70. https://doi.org/10.1016/j.postharvbio.2018.12.012.
Laguerre, O., Denis, A., Bouledjeraf, N., Duret, S., Bertheau, E.D., Moureh, J., Aubert, C., Flick, D., 2022. Heat transfer and aroma modeling of fresh fruit and vegetable in cold chain: Case study on tomatoes. Int. J. Refr. 133, 133–144. https://doi.org/10.1016/j.ijrefrig.2021.10.009.
Linke, M., Praeger, U., Mahajan, P.V., Geyer, M., 2021. Water vapour condensation on the surface of bulky fruit: Some basics and a simple measurement method. J. Food Eng. 307, 110661. https://doi.org/10.1016/j.jfoodeng.2021.110661.
Praeger, U., Jedermann, R., Sellwig, M., Neuwald, D.A., Hartgenbusch, N., Borysov, M., Truppel, I., Scaar, H., Geyer, M., 2020. Airflow distribution in an apple storage room. J. Food Eng. 269, 109746. https://doi.org/10.1016/j.jfoodeng.2019.109746.
Singh, R.P., Heldman, D.R., 2009. *Modes of heat transfer*. Introduction to food engineering, fourth ed. Academic press, Burlington San Diego London.
van der Sman, R.G.M., 2003. Simple model for estimating heat and mass transfer in regular-shaped foods. J. Food Eng. 60, 383–390. https://doi.org/10.1016/S0260-8774(03)00061-X.
Wakao, N., Kaguei, S., 1982. Heat and mass transfer in packed beds. Gordon and Breach, New York.
Wu, W., Cronjé, P., Verboven, P., Defraeye, T., 2019. Unveiling how ventilated packaging design and cold chain scenarios affect the cooling kinetics and fruit quality for each single citrus fruit in an entire pallet, 21. Food Packaging and Shelf Life, 100369. https://doi.org/10.1016/j.fpsl.2019.100369.
Wu, D., Shen, J., Tian, S., Zhou, C., Yang, J., Hu, K., 2018. Experimental study of temperature characteristic and energy consumption of a large-scale cold storage with buried pipe cooling. Appl. Therm. Eng. 140, 51–61. https://doi.org/10.1016/j.applthermaleng.2018.05.035.